Analysing Digital In-Memory Computing for Advanced FinFET node

Veerendra S Devaraddi*, Joycee M. Mekie†
*International Institute of Information Technology Bangalore
†Indian Institute of Technology Gandhinagar

***Abstract*—Digital In-memory computing improves energy efficiency and throughput of a data intensive process, which incur memory thrashing and, resulting multiple same memory accesses in a von Neumann architecture. Digital in-memory computing involves accessing multiple SRAM cells simultaneously, which may result in a bit flip when not timed critically. Therefore we discuss the transient voltage characteristics of the bitlines during an SRAM compute.**

To improve the packaging density and also avoid MOSFET downscaling issues, we use a 7-nm predictive PDK which uses a finFET node. The finFET process has discrete fins and a lower Voltage supply, which makes the design of in-memory compute SRAM difficult. In this paper, we design a 6T SRAM cell in 7-nm finFET node and compare its SNMs with a UMC 28nm node implementation. Further, we design and simulate the rest of the SRAM peripherals, and in-memory computation for an advanced finFET node.

***Index Terms*—finFET, SRAM, In-memory computation, Latch-based sense amplifier, compute dynamic characteristics.**

I. Introduction

As the need and possibilities of Machine Learning increase, its usage in servers to portable devices increases. It being a data-intensive process and therefore incurs memory thrashing because of large data size and lack of frequent reusability of data in the cache of a von Neumann architecture. As a result of memory thrashing, throughput and energy efficiency reduces. In-memory computing addresses the issues to provide higher throughput and energy efficiency.

As the demand for higher performance increases, industries demand higher packaging density solutions. It leads to downscaling of channel length in MOSFETs, which leads to short-channel effects and high leakage current. Thus by restructuring the gate in a MOSFET, finFET is developed to have higher electrostatics control over the channel. SRAM, which occupies the most area on a die, is designed using a 7-nm predictive PDK to achieve higher packaging density.

A 6T-compute SRAM memory has 6T bit cells, sense amplifier, write driver, precharge circuit and compute logic in each column of the compute SRAM. In this paper, we consider 128 bit cells in each column of the compute SRAM.

II. 6T SRAM cell

A 6T SRAM cell consists of two cross-coupled inverters with two access transistors. To enable successful read, pulldown transistors(D) are designed to be stronger than the access transistors(A) and to enable successful write, the access transistors(A) are designed to be stronger than the pullup transistor(P). The relative strength of these transistors affect the read and hold stability, and write-ability of the 6T cell. We define the ratio of widths of pulldown transistor(D) to the access transistor(A) as *beta ratio*. Similarly the ratio of widths of pullup transistor(P) to the access transistor(A) as *pullup ratio*. As the absolute difference in the strength of the pulldown(D) and pullup(P) transistors increases, hold stability of the 6T cell decreases. Therefore beta ratio and pullup ratio are decided based on the application and overall simulation results.

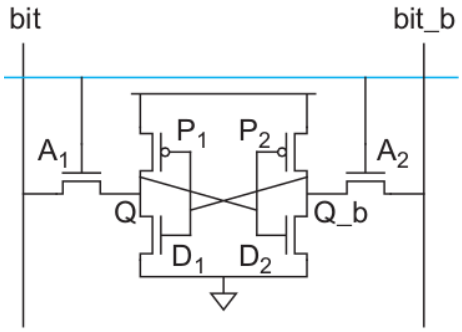

Fig. 1. 6T SRAM cell

The stability and write-ability of the cell are quantified using *static noise margin* (SNM). The SNM measures how much noise can be applied to the inputs of the two cross-coupled inverters before a stable state is lost.

A. Hold SNM

6T cell in a hold state is neither read nor written. Hold margin is obtained by plotting the voltage characteristics of both inverters. The SNM is determined by the length of the largest square that can be inscribed in the plot. As the VDD decreases the hold margin decreases and as the absolute difference in the strength of the pulldown(D) and pullup(P) transistors increases, hold SNM of the 6T cell decreases.

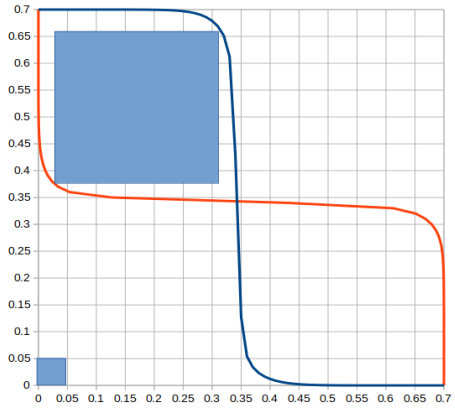

Fig. 2. Voltage characteristics of cross-coupled inverters for hold state

B. Read SNM

6T cell in a read state is accessed through the access transistors, and the bitlines are charged to VDD. An extreme case while reading is created when both the bitlines are at VDD. Hence read SNM is obtained by plotting the voltage characteristics of both inverters, with the access transistors turned on and the bitlines are connected to VDD. The SNM is determined by the length of the largest square that can be inscribed in the plot. As the beta ratio increases, the read margin increases.

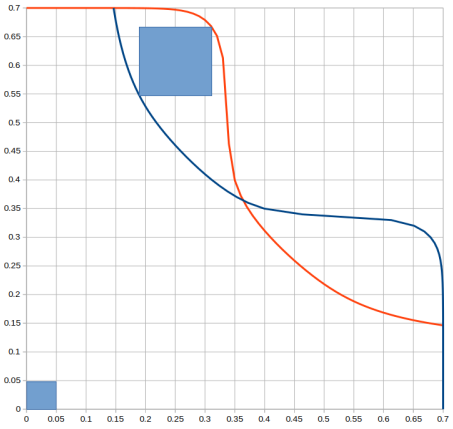

Fig. 3. Voltage characteristics of cross-coupled inverters for read state

C. Write SNM

6T cell in a write state is accessed through access transistors, and one of the bitlines is connected to the ground and the other bitline is connected to VDD. Hence write SNM is obtained by plotting the voltage characteristics of both inverters, with access transistors turned on, and one of the bitline is connected to the ground and the other bitline is connected to VDD. SNM is determined by the length of the smallest square that can be inscribed in the plot. As the pullup ratio increases, the write margin decreases or write-ability decreases.

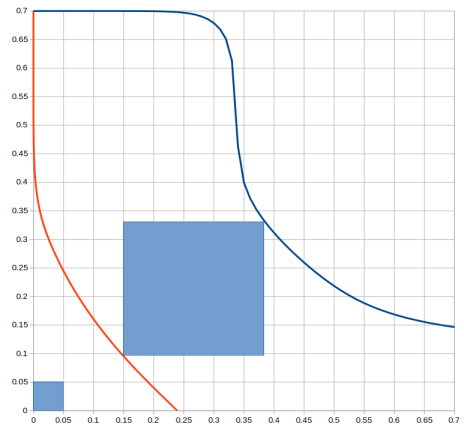

Fig. 4. Voltage characteristics of cross-coupled inverters for write state

D. SNM comparison between the 6T cell for a 7nm finFET node with VDD = 0.7V, and a 28nm UMC node with VDD = 0.9V

TABLE I
6T CELL SNM COMPARISON

Cell State	Static noise margin (mV)	
	7nm finFET node, VDD = 0.7V	***28nm UMC node, VDD = 0.9V***
Hold	284.09	328.92
Read	123.14	136.1
Write	234.38	305.66

III. SENSE AMPLIFIER: LATCH-BASED

Sense amplifiers are used to sense the voltage difference across the bitlines and produce a digital output. INN and INP of the sense amplifier are connected to bitlines of an SRAM column. Due to local variations, sense amplifiers give correct output if the absolute voltage difference across INN and INP is more than an offset voltage V_o. Sense amplifiers are the bottleneck during the operation of an SRAM. Therefore it determines the speed of the SRAM. The total sensing time is expressed as a sum of bitline discharge time T_o and sense amplifier latch time T_{latch}.

$$T_{total} = T_o + T_{latch} \tag{1}$$

T_{latch} is the time required by the sense amplifier to give an output once it is enabled. T_o is the time required to discharge the bitlines, which are charged to VDD initially, to a voltage difference of V_o across them. T_o *dominates* the total delay as the size of the memory and offset V_o increases [1]. Therefore we expect the offset voltage V_o to be as small as possible.

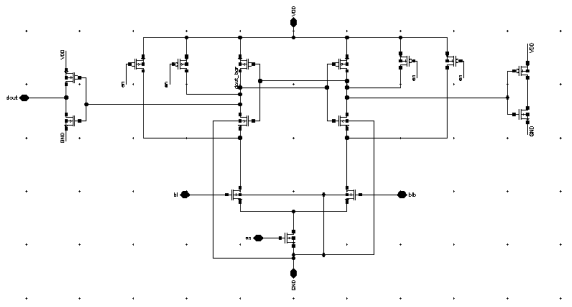

Fig. 5. Latch-based sense amplifier, with buffer for added robustness and predictability

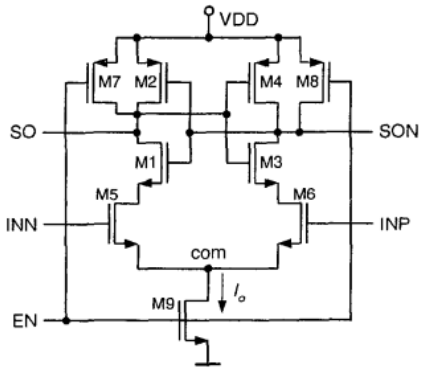

Fig. 6. Latch-based sense amplifier

A. Analysis of latch based sense amplifiers

SO and SON are charged to VDD when the sense amplifier is disabled(EN=0). As soon as the sense amplifier is enabled(EN=1), SO and SON starts discharging. Based on the voltages of INN and INP, either one of them starts discharging at a faster rate. As soon as the faster discharging node(either SO or SON) reaches a voltage which is lesser than the point of intersection in the transfer characteristics of the cross-coupled inverter in the sense amplifier(Example Fig. 2), the sense amplifier latches the output.
Since the strength of pull-up transistor(M2,M4) with respect to pull-down transistor(M1,M3) determines the point of intersection in the transfer characteristics of the cross-coupled inverter in the sense amplifier. The strength of pull-up transistor is increased with respect to pull-down transistor, to decrease the latch delay T_{latch}, but this makes the sense amplifier more vulnerable to noise and variations.

B. Offset voltage V_o calculation

Typically offset V_o is determined by a Monte-Carlo simulation, which statistically provides an offset voltage. Due to the unavailability of Monte-Carlo simulation in the 7-nm predictive PDK at the *time of this analysis*, the offset voltage is determined by considering M6 in FF corner and M5 in TT corner during simulation, which is a worst case. The difference between INN and INP is increased until SON becomes digital one. The voltage difference at which SON becomes digital one is added with necessary margin to determine the offset voltage V_o.

C. Results

After determining T_o and T_{latch}, the maximum operational frequency of pre-clock achieved is, more than 10GHz.

IV. Precharge

A Precharge circuit is used to charge the bitlines so that bit flip is avoided. This is done because the pullup transistors in a 6T cell is weaker as compared to the access transistors and therefore precharging the bitlines reduces the current through the pullup transistor and avoids saturation of the the pullup transistor. The transistors are sized such that the bitlines get sufficiently charged within half of the pre-clk cycle.

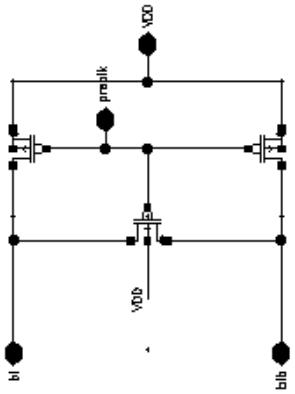

Fig. 7. Precharge circuit

V. Write Driver

Write driver is used to write a bit in a 6T SRAM cell. Write driver pulls one of the bitlines to VDD and the other bitline to the ground to bring the 6T cell to a required stable state(i.e Q=0 or 1). A 6T cell is designed such that pullup transistors are weaker than the access transistors, which makes writing to the 6T cell easier. The transistors are sized such that the bitlines are pulled to respective voltages sufficiently earlier, to ensure reliable writing. That is within half of the pre-clk cycle.

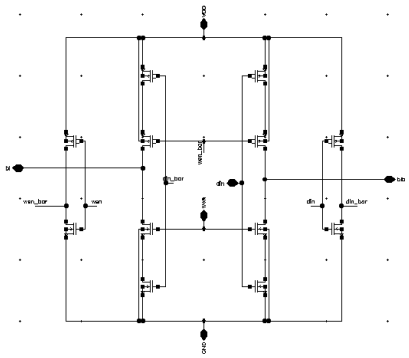

Fig. 8. Write Driver

VI. SRAM READ/WRITE SIMULATION

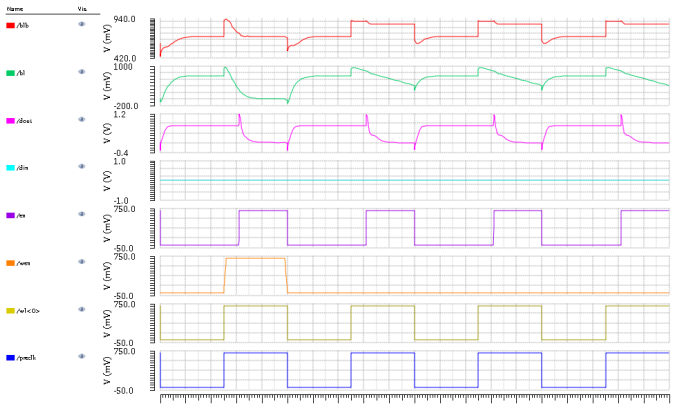

Fig. 9. Read/Write simulation on a 128 bit SRAM column

VII. DIGITAL IN-MEMORY COMPUTATION

In this section, we analyse the transient voltage of bitlines and discuss the compute logic to enable reliable and high speed computation. That is, a digital compute in a *pre_clk* cycle in each column of the compute SRAM.

A. Bitlines Transient Voltage Characteristics

During an SRAM compute, the bitlines are precharged to VDD initially, and then two 6T cells are accessed in each column of SRAM simultaneously. In this phase, the bitlines transient voltage is analysed to come up with timing constraints to enable reliable and high speed computation.
If A and B are the bits stored in the 6T bit cells that are involved in a computation, then bitline transient voltage during a compute in SRAM can be categorized into two types:

1) $A = B$: In this case, the bits stored in the two 6T bit cells are the same. A bitline is connected to both ”0”s, and the other bitline is connected to both the ”1”s. The bitline discharge is therefore similar to an SRAM read bitline discharge. The bitline discharge is faster than the SRAM read bitline discharge. Therefore this case of computation does not add any constraints over the SRAM read constraints.

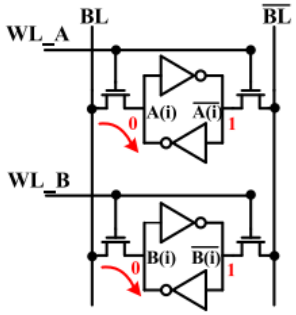

Fig. 10. Bitline transient voltage during a compute in SRAM for $A = B$ case [2]

2) $A = \overline{B}$: In this case, the bits stored in the two 6T bit cells are complimentary. The bitlines are connected to a ”1” and a ”0”. The discharge of bitlines is divided into two phases.

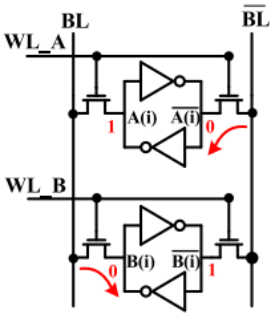

Fig. 11. Bitline transient voltage during a compute in SRAM for $A = \overline{B}$ case [2]

Figures 11 and 12 are showing the two phases of bitlines discharge during a compute in SRAM for $A = \overline{B}$ case. M1 and M2 are denoting the access transistors of two 6T cells involved in a computation.

Initially, the bitline is precharged to VDD and therefore, the source-to-drain voltage of M1 is close to zero and as a result, the current through M1 is also smaller. The source-to-drain voltage of M2 is close to VDD and as a result, the current through M2 is larger than the current through M1. Hence, the bitline voltage initially decreases from VDD.

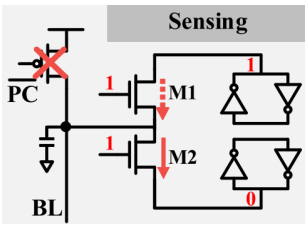

Fig. 12. Initial bitline voltage characteristics during compute, $A = \overline{B}$ [2]

Subsequently, as the bitline voltage decreases from VDD, the source-to-drain voltage of M1 increases and the source-to-drain voltage of M2 decreases. Therefore the current through

M1 increases. Eventually, the *pullup* transistor of "1" bit 6T cell gets into saturation region, because the design of a 6T cell is such that pullup transistors are the weakest transistors in the 6T cell. As a consequence, the voltage at the drain of the pullup transistor(or output of cross-coupled inverter) reduces significantly, resulting in a bit flip of the original "1" bit 6T cell.

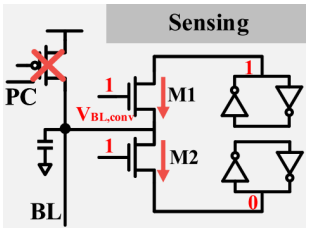

Fig. 13. Subsequent bitline voltage characteristics during compute, $A = \overline{B}$ [2]

Similar transient voltage characteristics is observed on the other bitline.

B. Discussion

To avoid the bit flip during bitline voltage dynamics, a Monte-Carlo simulation is done to come up with a time constraint such that the pullup transistor of 6T cell does not get into the saturation region and thus the bit flip is avoided.

C. Sense amplifier for computation

A sense amplifier is used for each bit line i.e two sense amplifiers in each column of the compute SRAM. Each sense amplifier takes two sensing inputs: a bitline and a reference voltage V_{ref}. V_{ref} value is determined such that the outputs of the two sense amplifier are A.B (AND) and A+B (OR).

D. Compute logic

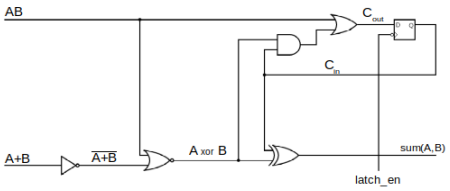

Fig. 14. Compute logic

A.B and A+B are used to produce the sum of A and B and the carryout. Therefore primary operations are AND, OR, NOR, XOR, NAND, XOR and SUM with carryout. These primary operations are used to perform complex operations [3].

E. Bit-serial and Bit-wise operation configuration

Bit-wise operations operate on all the bit places of the operands at the same time, the result of a bit place does not affect the result of other bit places. Bit-serial operations operate on a single bit at a time and its result influences the result of other bit places.

To do a Bit-wise operation, bits of the operand are stored along the row and each operand is in a different row of the compute SRAM. The operation occurs on all the bits of the operands at the same time. Therefore the latency is the same as for a single bit operation.

To do a Bit-serial operation, bits of the operands are stored along the column and both the operands are in the same column. That is bits of operand1 are stored along a column, then the bits of operand2 are also stored along the same column. The operation occurs on a single bit place at any time. Therefore the latency for a bit-serial operation is N cycles where N is the bit width of operands. Since the operands are stored in a single column, M bit-serial operations are done in parallel where M is the number of columns in the compute SRAM.

F. Example of A.B and A+B on two 6T cells with 1 and 0 stored in them

dout0 and dout1 represent A.B and A+B respectively, in the last pre-clk cycle.

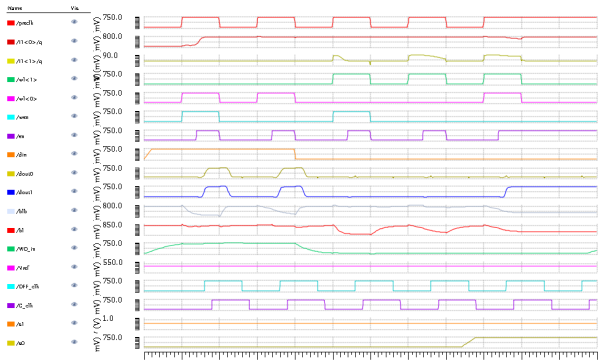

Fig. 15. An example compute

VIII. Summary and Conclusion

In this paper, we have designed a 6T SRAM cell for an advanced 7-nm finFET node and compared it with a 28-nm UMC node. We also presented the design flow of an SRAM by designing the peripherals of the SRAM for the finFET node. We analysed the transient voltage characteristics of bitlines to achieve a high speed and reliable computation in SRAM. We also discussed the modifications to *sense amplification* so that we get the required outputs from the sense amplifiers. We discussed the compute logic, that is present in each column of the compute SRAM. We also discussed operand storage configurations, to perform either bit-wise and bit-serial operations.

After all the analysis, we have come up with the timing constraints and the reference voltage for the sense amplifiers. This rest of the SRAM peripherals can be implemented to enable standalone operation of in-memory compute SRAM.

IX. Acknowledgement

I would like thank IIT Gandhinagar for organizing the Summer Research Internship Program, which enabled this project.

I would like to thank my advisor Prof. Joycee M. Mekie and my mentor Mr. Kailash Prasad from IIT Gandhinagar.
I would like to thank Prof. Nanditha Rao from IIIT Bangalore for the constant support and help.

REFERENCES

[1] B. Wicht, T. Nirschl and D. Schmitt-Landsiedel, "A yield-optimized latch-type SRAM sense amplifier," ESSCIRC 2004 - 29th European Solid-State Circuits Conference (IEEE Cat. No.03EX705), 2003, pp. 409-412, doi: 10.1109/ESSCIRC.2003.1257159.

[2] J. Chen, W. Zhao, Y. Wang and Y. Ha, "Analysis and Optimization Strategies Toward Reliable and High-Speed 6T Compute SRAM," in IEEE Transactions on Circuits and Systems I: Regular Papers, vol. 68, no. 4, pp. 1520-1531, April 2021, doi: 10.1109/TCSI.2021.3054972.

[3] J. Wang et al., "A 28-nm Compute SRAM With Bit-Serial Logic/Arithmetic Operations for Programmable In-Memory Vector Computing," in IEEE Journal of Solid-State Circuits, vol. 55, no. 1, pp. 76-86, Jan. 2020, doi: 10.1109/JSSC.2019.2939682.